

DRAFT

SENSITIVITY STUDY OF EULERIAN MULTIPHASE BOILING MODELS: NPHASE-CMFD

I. Asher¹, K. Fidkowski¹, T. Drzewiecki², T. Grunloh²,
V. Petrov², A. Manera², and T. Downar²

¹ Univ. of Michigan Dept. of Aerospace Engineering, 1320 Beal Ave., Ann Arbor, MI, USA

² Univ. of Michigan Dept. of Nuclear Engineering, 2355 Bonisteel Blvd., Ann Arbor, MI, USA

isaaca@umich.edu, kfid@umich.edu, tjdrzew@umich.edu, grunloh@umich.edu, petrov@umich.edu,
manera@umich.edu, downer@umich.edu

ABSTRACT

Reliance on multiphase fluid-dynamics models, which are developed with relatively limited experimental data, requires a quantitative assessment of the solution variability due to the approximations. In this paper, uncertainty in the Eulerian multiphase boiling model in the Nphase-CMFD code is assessed in the context of the DEBORA test case and the CRUD problem. The models under consideration are turbulence, wall-boiling heat transfer, bulk flow heat transfer, dispersed phase characterization, and interfacial momentum transfer. Experimental and numerical data are compiled to formulate reasonable ranges for the model parameters of interest. This is done in the context of a larger effort to compare various multiphase codes, including Star-CD and Star-CCM+, and various physical setups. The Nphase-CMFD code was moderately coupled to Star-CD in order to meaningfully compare the codes. For parameter ranges based on the available literature, the bubble diameter and turbulent dispersion coefficient were found to have the largest effect on the outputs of interest for the CRUD problem. Although it is well known that the constant bubble diameter in Nphase-CMFD is a poor approximation, the turbulent dispersion coefficient is not usually considered to be important. The results underscore the need for comprehensive uncertainty quantification and further development of some multiphase models.

1. INTRODUCTION

Models for boiling and two-phase flows, particularly in the subcooled regime, are important for thermal hydraulics simulations that support safety and performance analyses of nuclear reactors. Numerous models are currently available for such simulations, e.g. [1,2], many with first-principles justifications [3], but each with a certain number of parameters that can be regarded as tunable or empirically-based. In some cases, these models do not give the same answers and do not necessarily correlate to experiments if they are not independently adjusted for the particular case of interest. A documented example is the failure of high-pressure models applied to subcooled boiling at low pressures [4].

The objective of this study is to quantify many of the uncertainties in thermal hydraulics models by systematically computing global sensitivities of figures of merit, or outputs, to model parameters. These sensitivities are used to identify parameters that are important for the prediction of the outputs of interest, allowing for a reduction of the input-space dimensionality in future applications such as

uncertainty propagation and reliability analysis. Furthermore, by using parameter ranges that reflect the physical variability of the models, critical parameters can be identified as important targets for model improvements.

Previous works have considered the sensitivity of boiling models to inputs parameters and sub-models. Tu and Yeoh [5] studied subcooled boiling at low pressure using Ansys CFX and found that parameters pertaining to partitioning of the wall heat flux, the mean bubble diameter, and the bubble departure diameter have a strong effect on the void fraction. Koncar and Krepper [6] used Ansys CFX to investigate boiling of a refrigerant in turbulent subcooled boiling, for which sufficient mesh resolution, the correct bubble diameter, and the inclusion of the bubble lift force were found to be important for ensuring accurate validation.

This sensitivity study proceeds by choosing representative boiling and two-phase flow models in the Eulerian Multiphase CFD code Nphase-CMFD [7]. The DEBORA test case, which consists of subcooled boiling in a straight channel geometry with simple boundary conditions, is the benchmark problem that drives this study. Nphase-CMFD is weakly coupled to and compared to another multiphase code, Star-CD. The Star-CD code has been used for validating subcooled boiling models in previous work [8]. In addition, the authors have investigated parameter sensitivities in Star-CD for the DEBORA test case [9]. Therefore, comparisons between the codes help to separate uncertainty due to the multiphase models themselves from that due to the implementation.

First, a set of numerical investigations is done to set up the baseline parameters and mesh, using the Star-CD solution and experimental data as references. Next, a preliminary sensitivity study is performed to assess the coupling between Nphase-CMFD and Star-CD. In the main sensitivity study, ten input parameters pertaining to many of the empirical models are varied via a Latin-Hypercube Monte-Carlo approach using the software package DAKOTA. The scalar outputs of interest in the present study are the pressure drop in the channel, the average wall temperature, the average void fraction at one axial location, and the radial-centroid of this void fraction profile.

2. THE DEBORA TEST PROBLEM

The test problem consists of a heated circular pipe with R12 flowing vertically through it. The geometry is shown in Figure 1. We note that the system pressure is 1.459 MPa. The outputs of interest for the CRUD problem are the pressure drop over the pipe (Δp), average wall temperature (T_w), average void fraction at the measurement location (α_g), and radial centroid of the void fraction profile at the measurement location (r_a). Experimental data are available in the form of the void fraction profile at the measurement location.

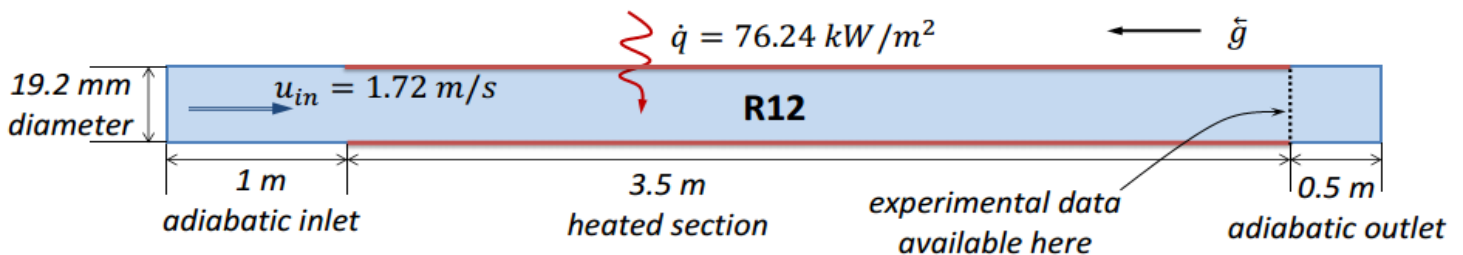


Figure 1. The DEBORA test case. The cross-section is circular and the simulation is performed with the axi-symmetric assumption.

3. NPHASE-CMFD CODE

3.1. Model Choices

Developed at RPI, Nphase-CMFD is a finite volume, parallel multiphase fluid dynamics solver that can handle two-and three-dimensional unstructured grids and an arbitrary number of phases. Many built-in multiphase models are available, and user defined C-subroutines, with access to all data structures in the code, allow much flexibility in the specification of mass, momentum, and heat transfer models. In this work, a high-Reynolds number k - ϵ model is used for the liquid phase. The pressure drop between the phases is negligible. A simple version of the wall force is implemented by setting the lift force to zero near the wall. The drag coefficient is based on the Wang curve fit [10], which is used by Star-CD. The heat transfer between phases is computed using two Nusselt number correlations: the modified Ranz-Marshall for liquid-interface transfer [11], and a correlation developed at RPI based on transient bubble growth and decay for gas-interface transfer [12]. It should also be noted that the gas phase was set at a constant enthalpy slightly above the saturation enthalpy (D.R. Shaver, personal correspondence, Jan. 2012).

3.2 Bubble Diameter

A single, fixed bubble diameter was used for the entire computational domain. While many classes of bubbles can be specified, transfer models are needed for each equation and population pair, and this would render the model quite difficult to implement and would be very different from the model used in Star-CD. At the time of the investigation, Nphase-CMFD did not allow an S-Gamma formulation for the bubble size distribution, and a single, fixed bubble size was used because it was the default bubble population model.

In the Nphase solution, the bubble diameter was fixed at $7e-4$ m. This value was chosen by visually inspecting the Star-CD solution. The converged temperature distribution was used to calculate the bubble diameter that Star-CD would have used based on the its $d(T)$ correlation [13], which gave d in the range [$1.5e-4$, $18.46e-4$] with an average of $6.35e-4$ m (note, this correlation for d was used in the previous Star-CD study [9]). Thus, the fixed value gives a relatively good estimate of the average bubble diameter, given the large range of d in the Star-CD solution. The sensitivity study will determine if this range of d has a significant influence on the solution and the outputs of interest.

3.3 Wall Boiling

Special consideration also had to be given to the wall-boiling model. At the time of this work, there was no default model to partition the heat flux between the phases and the interface. Therefore, the user had to prescribe this wall heat partitioning. In this case, the Star-CD solution was used as a reference. Star-CD uses the Kurul-Podowski heat partitioning model, and the reference solution uses default values for parameters like bubble departure diameter, departure frequency, etc. Using the Star-CD heat partitioning for the Nphase solution couples the two codes together. Determining the strength of this coupling and the accuracy to which it must be resolved is discussed below.

In this study, as in the Star-CD heat partitioning model, we set the gas heating to zero. That is, any heat that does not cause liquid heating will generate vapor. This can be a problem if the void fraction reaches 1.0, since then any excess heat that goes into gas generation is ignored and effectively lost. Thus, we must ensure that during the solution process, none of the cells (especially near the heated wall) reach a void fraction of 1.0.

In order to have a realistic solution, we set the heat partitioning profile to the profile from the Star-CD DEBORA solution, which is shown in Figure 2. The profile was taken from Star-CD run on a uniformly spaced 800x20 (axial x radial resolution) mesh with absolute residuals converged below $1e-5$. The profile, which ranges from 0% to about 70% of the heat going to gas generation, was fitted by hand with three quadratics. The resulting fit had an estimated L_2 error of 2.25 percentage points.

Gas generation in Nphase requires specifying a porous wall and injecting the gas with a small velocity. The precise velocity is not important, as long as it does not affect the overall momentum balance. The actual condition that is enforced is the imparted mass flux. The chosen velocity of $7.45e-2$ m/s was verified to not significantly affect the momentum balance (specifically, this contributes an additional 0.016% to the overall momentum at the wall).

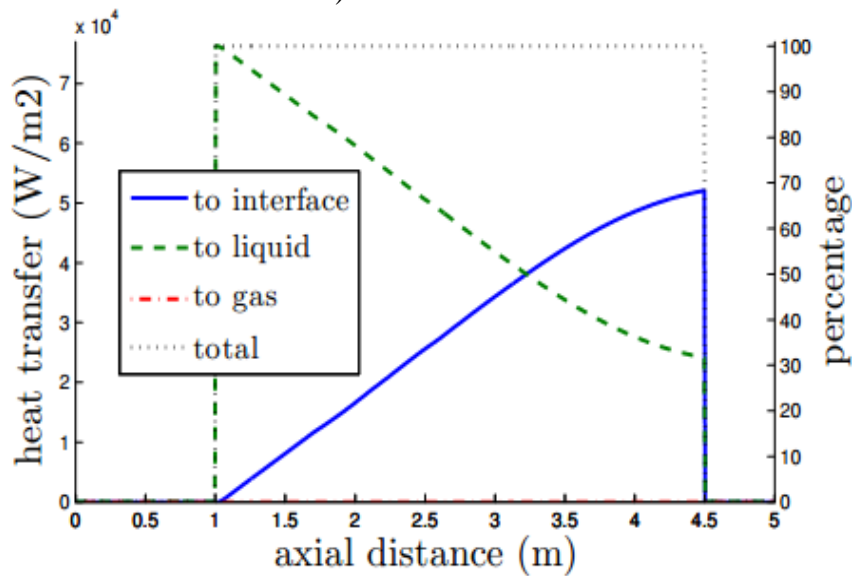


Figure 2. Heat partitioning profile from Star-CD DEBORA solution.

The above model choices, along with default values for other models [7], allows for a baseline solution that is similar to the Star-CD solution and facilitates comparisons between the codes.

4. COMPUTATIONAL MESH

The computational mesh was a 2D, axisymmetric, structured mesh. Solutions were found using both the low-Re and high-Re turbulence models, which require different meshes. For the low-Re model, the mesh must resolve the entire viscous sublayer near the wall. For the DEBORA test case, this results in a very small grid spacing near the wall of $1.5e-6$ m which gives a y^+ slightly below 1.0 for the converged solution.

For the high-Re model, a much coarser mesh is possible, since we require the mesh spacing near the wall to have a $y^+ > 50$. A spacing of $4e-4$ m results in $50 < y^+ < 80$ for the converged solution. The mesh had 30 cells in the radial direction and 400 axially, which was deemed sufficient resolution for engineering accuracy by inspection of the solution and outputs on a few different mesh resolutions. The only quantity that varies rapidly with respect to mesh spacing is the radial velocity, where there seems to be a discontinuity at the end of the heated section. In this work, we did not have time to investigate this feature or if resolving it significantly changes the solution. However, we have

encountered numerous cases in which the radial velocity distribution is strongly affected by parameters that otherwise have little or no effect on the solution. Thus, we assume that resolving the (relatively small) radial velocity would not significantly change the solution. We should also note that the radial momentum equation almost always has the highest relative errors in converged solutions.

Although a solution on the low-Re mesh was converged, it was prohibitively expensive to do further tests or use it in the sensitivity study. The low-Re solution was used to verify the turbulence modeling, but all of the data and results in this report are based on the high-Re solution.

5. BASELINE SOLUTION

In order to arrive at a converged solution, we took a number of steps from simple flows to the final DEBORA case. At each stage, the solution from the previous stage was used as the initial condition. Before moving to the next stage, the solution at a given stage was converged as much as possible, until the state updates did not change in magnitude. The stages were as follows:

1. Compute the approximate, fully developed turbulent pipe flow solution using known profiles from the literature. Velocity and pressure fields were computed.
2. Solve for the single-phase, unheated pipe flow. The goal is to solve for the turbulent quantities.
3. Solve for multi-phase, heated pipe flow with full heat flux but mass flux reduced to 10% of nominal.
4. Slowly increase to full mass flux.

The recommended method for assessing convergence in Nphase is checking the magnitude of the state updates, specifically the root-mean-squared update (not taking into account the mesh spacing). Since each variable is scaled differently (e.g. pressure is on the order of 10e6 Pa, velocity around 1 m/s), the updates must be compared to the magnitude of the state. In this study, convergence was assessed using the ratio $RMS(update)/RMS(state)$, which was not originally available in the code. Also, rather than looking at each velocity component separately, we look for convergence of the magnitude of the velocity vector.

The convergence of the DEBORA solution while increasing the mass flux is shown in Figure 3. The root-mean-square of the state update (normalized by $RMS(state)$), is plotted for the seven states. Each spike in the plot represents an increase in the mass flux and a restarting of the solution. The enthalpy (“h”, the purple line) converges quite quickly, since the energy equation is linear. The pressure and turbulent quantities (“p”, “k”, and “e”) converge to the point where relative updates are around $1e-6$. The void fraction and velocity magnitude (“a” and “u”) do not converge as well, but relative updates are still less than 0.1%. Finally, the radial velocity component (“v”, the green line) has constant oscillations around 1%. This may be due to the discontinuous nature of the radial velocity profile, as seen in Figure 4. However, the small $RMS(\text{radial velocity})$, compared to that of the axial velocity, results in a heavily polluted convergence measure. Since the radial velocity component is not generally of much interest, the issue was not addressed further.

The final solution is plotted in Figure 4 and Figure 5. The calculation was done with an axisymmetric mesh, so only a cross section is shown. The top of the plot represents the wall of the cylinder, the bottom is the centerline, and the flow is from left to right. The inlet effects, boundary layer, and radial velocity feature at the end of the heated section are apparent in Figure 4. Even though the velocity at the cell adjacent to the wall is far from zero, the wall functions in the high-Re turbulence model enforce the correct boundary conditions. The heat transfer from the wall and the

bubbles generated are apparent in Figure 5. The temperature surpasses the boiling point of 331.3 K, so some bulk boiling occurs near the end of the heated section.

The void fraction is nearly constant close to the wall because the lift force is set to zero here. Further from the wall, the lift force causes the bubbles to migrate toward the center of the pipe. The baseline solution shown in Figure 5 uses a lift coefficient of -0.03 and the lift force is disabled within one bubble diameter from the wall ($y_{wall}=1$). The void fraction distribution is highly dependent on the chosen lift model and varies considerably between Nphase, Star-CD, and Star-CCM+. An experimentally determined void fraction profile is available at the end of the heated section, and Figure 6 shows that $C_L=-0.03$, compared to some other computational models, gives good agreement with the experimental data. The Star-CD and Star-CCM+ models have been somewhat tuned to the data (e.g. the virtual mass force is zero in Star-CCM+).

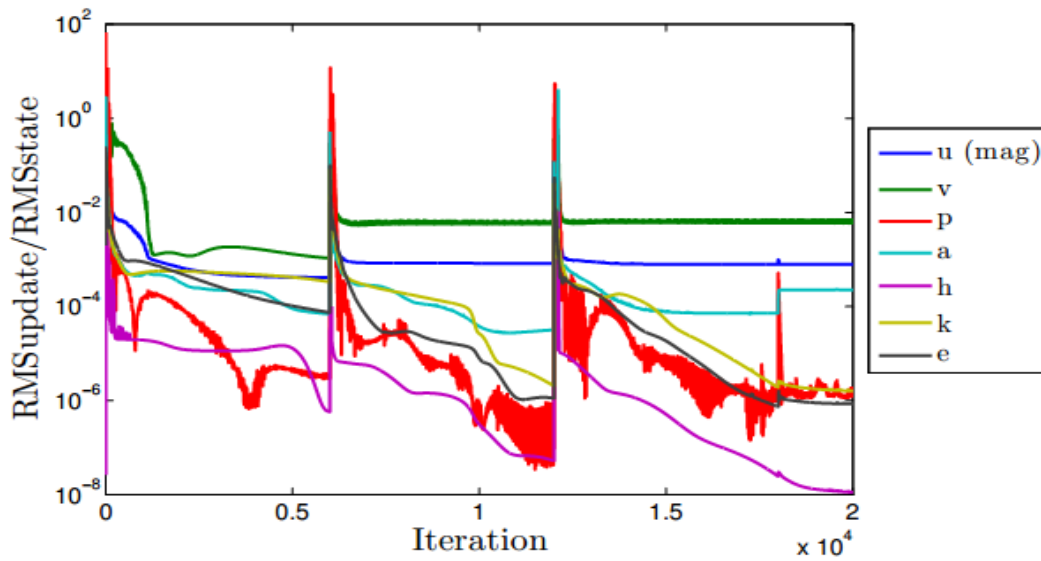


Figure 3. Convergence of baseline DEBORA solution in Nphase. Spikes occur when the wall mass flux is increased.

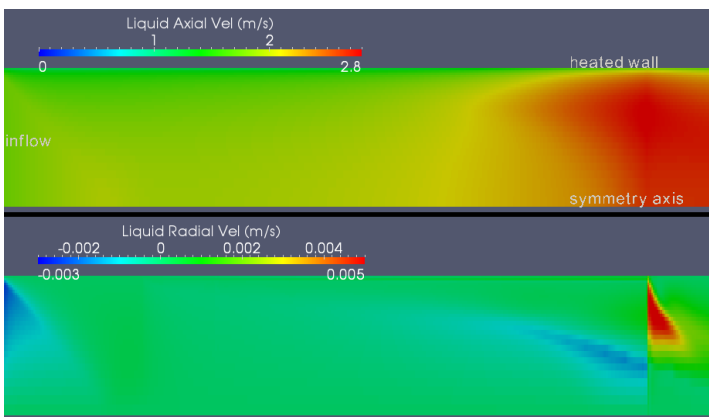


Figure 4. Baseline DEBORA solution in Nphase. Top is axial velocity, bottom is radial velocity of the liquid phase.

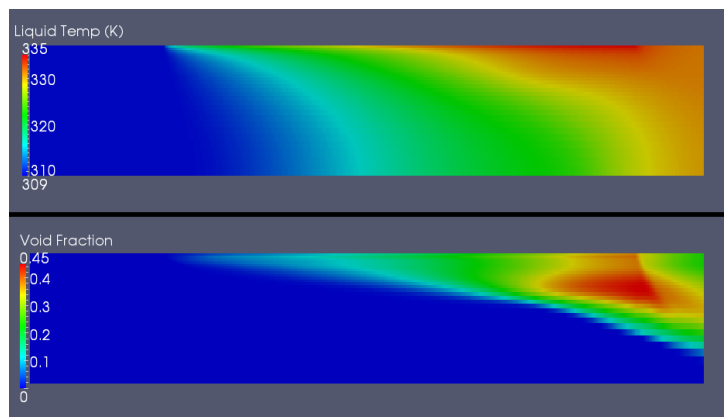


Figure 5. Baseline DEBORA solution in Nphase. Top is temperature of the liquid, bottom is void fraction.

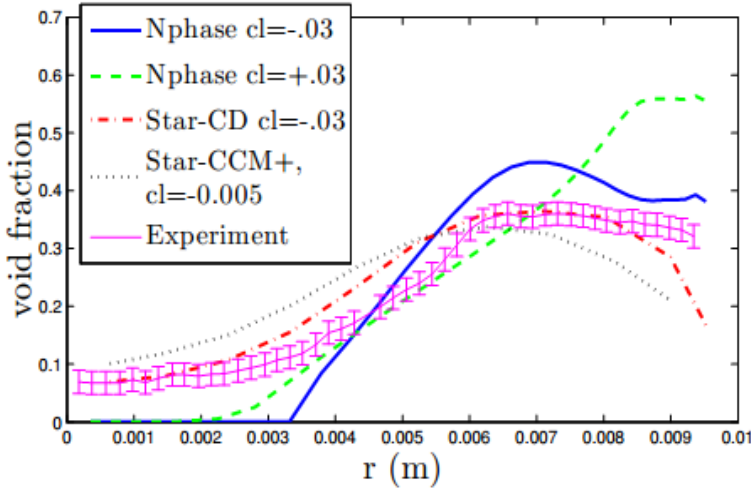


Figure 6. Comparison of void fraction profiles at the end of the heated section from various simulations and experimental data.

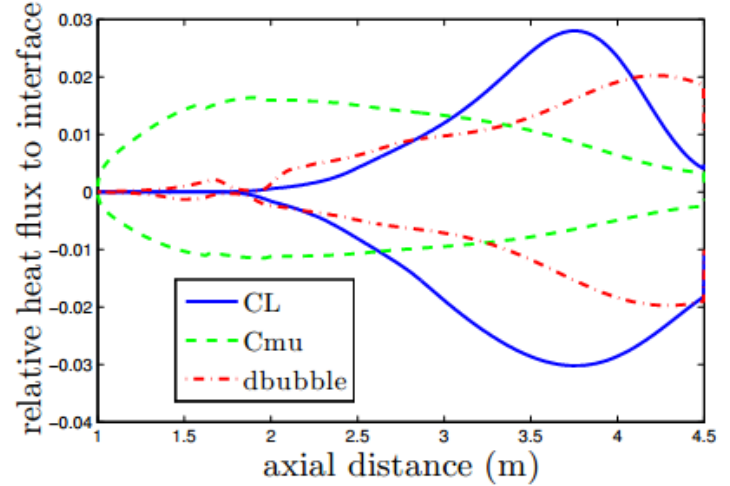


Figure 7. Variation of heat partitioning profile from Star-CD DEBORA solution, normalized to total heat flux.

6. STAR-CD COUPLING THROUGH HEAT PARTITIONING

Since a sensitivity study was performed, it was necessary to see if parameter variations modify the wall heat partitioning profile that was taken from the Star-CD solution. Parameters with the strongest effect on outputs were C_L , d_{bubble} , and C_{μ} . A centered parameter study was performed to assess variability in the heat partitioning profile. Although the values of C_L in the Star-CD sensitivity study were conservative ($-0.03 \pm 30\%$), we now wish to explore a larger range of C_L . The literature survey suggests that C_L should be in the range $[-0.3, 0.3]$, but Nphase does not converge well for $C_L > -0.01$. Table 1 shows the parameters and ranges, and Figure 7 shows the resulting profiles. If we define q_l as the heat flux going into the liquid and q_g as the heat causing boiling, then the plot shows

$$\left(\frac{q_g}{q_l + q_g} \right) - \left(\frac{q_g}{q_l + q_g} \right)_{baseline} = \widehat{q}_g - \widehat{q}_{g_{baseline}}$$

Thus, parameter variations cause at most a 3 percentage point change in the profile. This the same order of magnitude as the interpolation error encountered in importing the profile into Nphase.

Table 1. Parameters for sensitivity study of heat flux partitioning profile in Star-CD

Parameter	Range	Reasoning
C_L	$[-0.1, -0.01]$	Required for convergence
d_{bubble}	$\pm 30\%$	Used in previous Star-CD sensitivity study
C_{μ}	$\pm 30\%$	Used in previous Star-CD sensitivity study

In order to see the extent to which modified heat partitioning profiles affect the outputs of interest, Nphase was then run with the (four) heat partitioning profiles for the modified d_{bubble} and C_L . The parameters in Nphase remained at baseline; only the heat partitioning was changed. The resulting variation in the outputs is shown in Table 2. Previous work on the sensitivity of Star-CD showed that these variations in the outputs are small compared to variations in the outputs from directly altering parameters. Although the actual d_{bubble} in the Nphase study was varied from -80% to +185%, which could lead to large output variations, these would be attributed to uncertainty in d_{bubble} , not the heat

partitioning. Thus, it is sufficient to use the baseline heat partitioning profile for all Nphase runs, provided that output variations less than the percentages in Table 2 are deemed insignificant.

Table 2. Variation in Nphase outputs for different heat partitioning profiles.

	Δp	T_{wall}	α_g	r_a
C_L	0.03%	0.07%	2%	0.4%
d_{bubble}	0.005%	0.05%	0.4%	0.15%

7. FULL SENSITIVITY STUDY

The full sensitivity study was performed using the same baseline solution as before. The heat partitioning profile was fixed to the baseline profile from Star-CD. After a literature survey, ten high-level parameters and appropriate ranges were chosen as shown in Table 3. The study had 1474 useable data points, which is more than the 1024 required for a full 2^k factorial design. Each run in the study had 4000 iterations, and less than 8% of the runs diverged. The rest converged to the point where $RMS(update)/RMS(state) < 1\%$ for all states (except the radial velocity, for which we had looser requirements as explained earlier).

Table 3. Parameters and ranges for full sensitivity study.

Parameter	Symbol	Nominal	Range	Reasoning
Lift coefficient	C_L	-0.03	[-0.1, -0.01]	Required for Nphase convergence, [14]
Drag coefficient	C_D	Wang fit	$\pm 30\%$	Approximate experimental variation (no data for Wang fit itself) [15]
Virtual mass coefficient	C_{VM}	1.0	[0.5, 1.5]	Nominal values in Star-CD (see also [16]) and Nphase, and part of range from [17]
Turbulent dispersion coefficient	C_{TD}	2/3	[0.3, 1.5]	Encompasses much of range from [18] and calculated from Nphase solution using formula in [19]
Bubble diameter	d_{bubble}	7e-4 m	[1.5e-4, 20e-4]	Range from Star-CD, Star-CCM+, Nphase, and [18].
Lift force wall distance	y_{wall}	1	[1, 4]	Range for Star-CD, Nphase, and [14,19,20]
Turbulent viscosity scaling	C_μ	0.09	[0.07, 0.09]	Calculated for Nphase solution using formulas in [21-24]
Nusselt number: liquid to interface	Nu_l	Modified Ranz-Marshall	$\pm 30\%$	Approximate range for many experimental results [25-29]
Nusselt number: gas to interface	Nu_g	Analytic (see [12])	[0, 50]	Encompasses much of analytic form in [12], data from [30], and Star-CD.
Heat flux partitioning	\widehat{q}_g	From Star-CD solution	$\pm 5\%$	Heat partitioning sensitivity study (see above).

Figure 8 shows the correlation coefficients for the full sensitivity study. The plots clearly show that the bubble diameter and the turbulent dispersion coefficient have overwhelmingly large effects on the outputs, compared to the other parameters in the study. Interestingly, the bubble diameter has little

effect on the average wall temperature. Both of these models have relatively little experimental evidence, yet have significant impact on the outputs.

By contrast, the lift, drag, and virtual mass forces, turbulence model, and wall heat partitioning model have little effect on the outputs, although many of these models are also lacking in experimental evidence. The heat partitioning model does indeed have a small effect (accounting for only 1.3% of the variation in the wall temperature), so we can be confident that it was reasonable to use a single heat partitioning profile for the entire study. The liquid Nusselt number seems to have a moderate effect on all of the outputs, but this model has enough supporting evidence that time would be better spent improving other models.

Figure 9 shows some scatter plots for the various outputs. Over the ranges of the parameters, which were chosen to be within the experimental and modeling uncertainty, the output ranges are shown in Table 4. For those engineering applications that demand tighter bounds on the uncertainty, the models presented here are insufficient. The results from this study suggest that more sophisticated models for bubble diameter, such as single or multi-equation interfacial area transport models, are needed to accurately simulate two-phase flow. Also, more experimental work should be done to more carefully characterize the turbulent dispersion force.

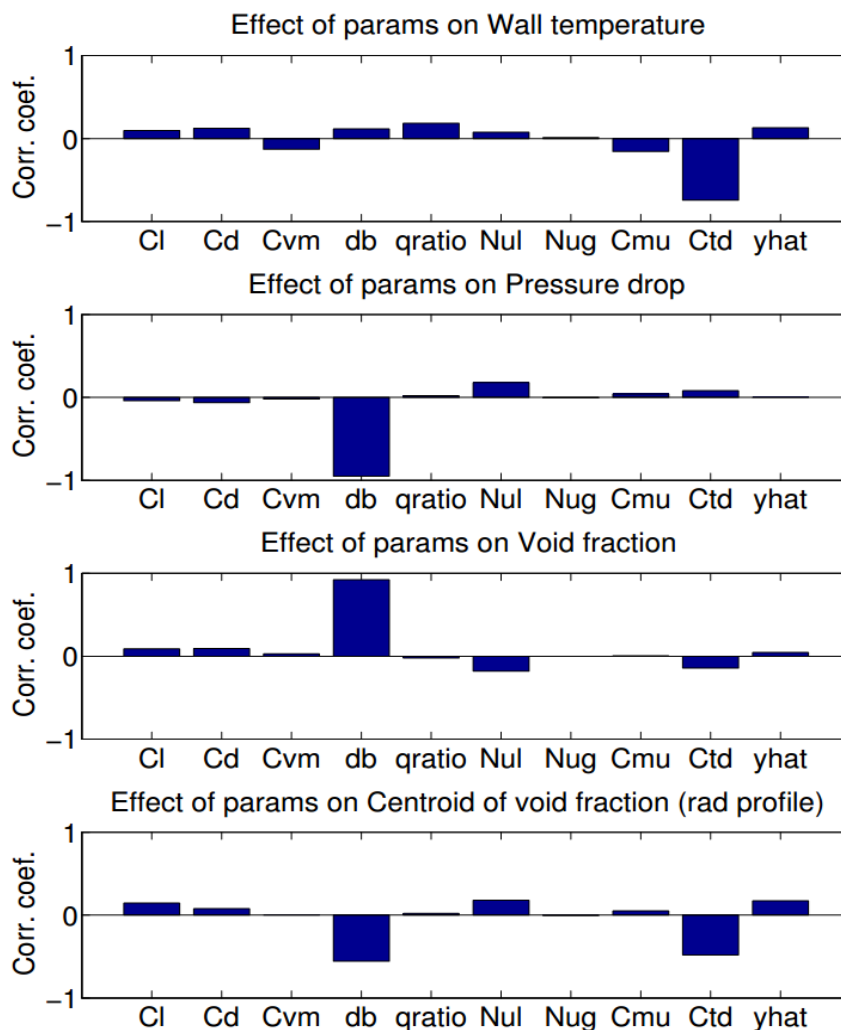


Figure 8. Correlation coefficients between parameters and outputs for the full sensitivity study.

Table 4. Overall output variations.

Δp	T_w	α_g	r_a
3.5 KPa (6%)	3.5 K (1%)	0.25 (77%)	2 mm (28%)

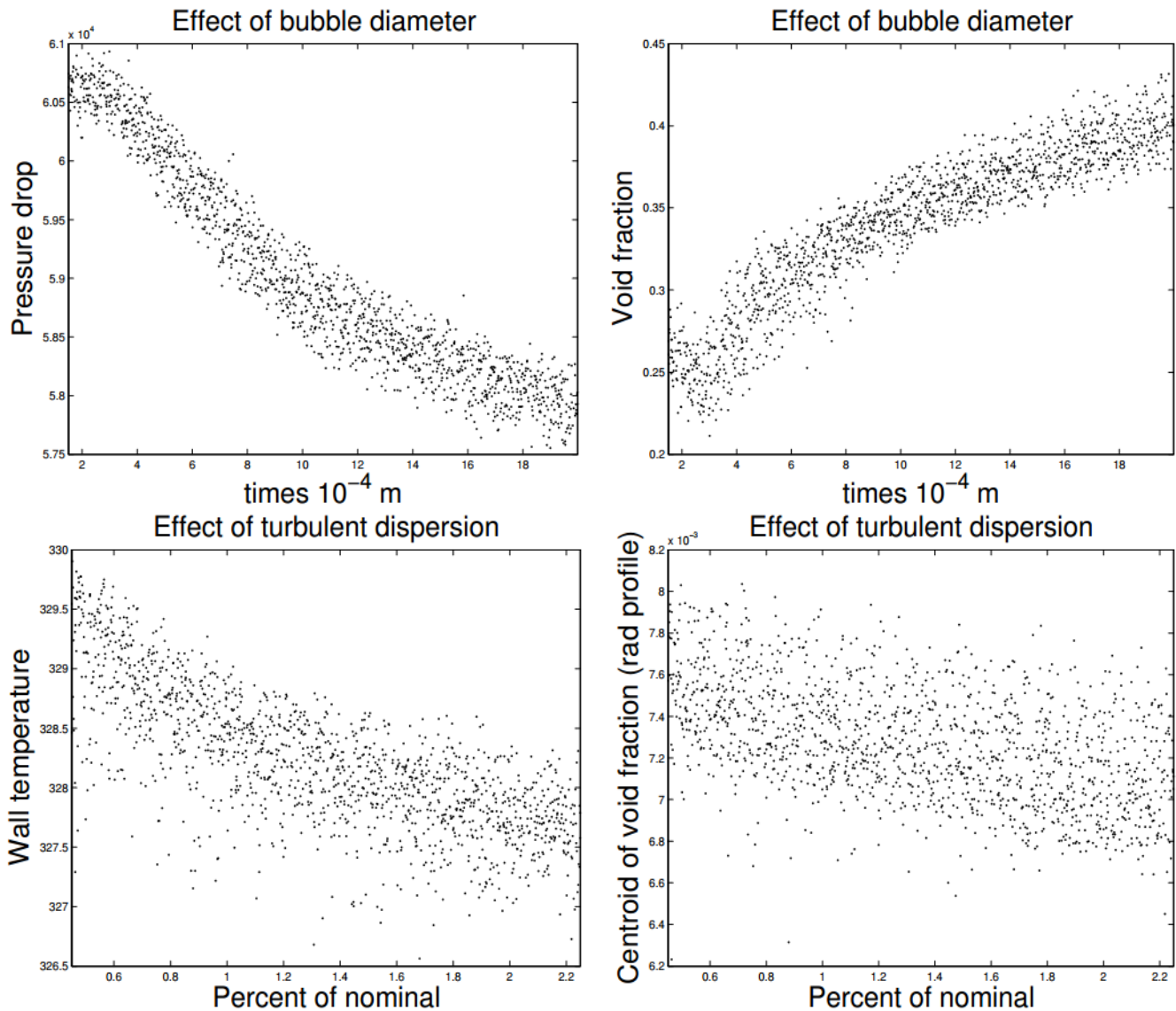


Figure 9. Example scatter plots for the full sensitivity study.

8. CONCLUSION

The models and data used in this study were limited in scope and only begin to address the overall problem of uncertainty quantification for multiphase models. The uncertainties associated with these models in other fluid regimes and physical setups require further investigation. We now give some conclusions regarding the uncertainties in simulating subcooled boiling channel flow with these models. First, the small effect of the heat partitioning ratio on the outputs implies that the complex wall boiling model used by Star-CD is not necessary to accurately predict the outputs considered here, and a simpler model may suffice. Second, the Star-CD sensitivity study highlighted the bubble departure diameter (at the boiling wall) as a very important parameter, and the current study highlighted the overall bubble diameter. Given the two results, it is likely that more accurate modeling

of the bubble diameter will improve the robustness of the two-fluid models used here. Third, the turbulent dispersion coefficient has very different models in Star-CD and Nphase. The large uncertainty due to the turbulent dispersion force in Nphase implies that the Star-CD model may be more precise and accurate, assuming it compares well with experiments. Fourth, the smaller effects of the Nusselt numbers and C_μ in Nphase compared to Star-CD probably reflects the $d(T)$ correlation used in Star-CD. Finally, it is interesting that the bubble lift force varies widely in the two sensitivity studies, but does not affect the outputs strongly in either case. During these investigations, it became clear that the lift force can strongly affect the stability of the system (i.e. sign of C_L , wall force). However, within the range of stable C_L , the actual value seems to have little effect on the outputs. Overall, both Star-CD and Nphase have somewhat large uncertainties for precise engineering applications. Both codes would benefit greatly from more accurate modeling of bubble sizes.

9. REFERENCES

- [1] N. Kurul and M.Z. Podowski, "On the modelling of multidimensional effects in boiling channels," ANS Proceedings, National Heat Transfer Conference, 1991.
- [2] R.M. Podowski and D.A. Drew and R.T. Lahey Jr. and M.Z. Podowski, "A mechanistic model of the ebullition cycle in forced convection subcooled boiling," Proceedings of the 8th International Topical Meeting on Nuclear Reactor Thermal-Hydraulics. Vol. 3, 1997.
- [3] M.Z. Podowski, "Recent development in the modeling of boiling heat transfer mechanisms," Proceedings of the 13th International Topical Meeting on Nuclear Reactor Thermal-Hydraulics, 2009.
- [4] G.H. Yeoh and J.Y. Tu "A bubble mechanistic model for subcooled boiling flow predictions," *Numerical Heat Transfer*, Vol 45, 2004, pp 475—493.
- [5] J.Y. Tu and G.H. Yeoh, "On numerical modelling of low-pressure subcooled boiling flows," *International Journal of Heat and Mass Transfer*, Vol 45, 2002, pp 1197—1209.
- [6] Bostjan Koncar and Eckhard Krepper, "CFD simulation of convective flow boiling of refrigerant in a vertical annulus," *Nuclear Engineering and Design* 238, 2008, pp 693—706.
- [7] Interphase Dynamics LLC. "Nphase-CMFD user manual, Nphase version 3.1.19." Technical Report, Rensselaer Polytechnic Institute, Sept 2009.
- [8] V. Ustinenko, M. Samigulin, A. Ioilev, S. Lo, A. Tentner, A. Lychagin, A. Razin, V. Girin, Ye. Vanyukov, "Validation of CFD-BWR, a new two-phase computational fluid dynamics model for boiling water analysis," *Nuclear Engineering and Design* 238, 2008, pp 660-670.
- [9] I.M. Asher, T.J. Drzewiecki, K.J. Fidkowski, and T.J. Downar. "Parameter sensitivity study of boiling and two-phase flow models in computational thermal hydraulics." 14th International Topical Meeting on Nuclear Reactor Thermalhydraulics, Toronto, Ontario, Canada, Sept. 2011.
- [10] D.M. Wang. "Modelling of bubbly flow in a sudden pipe expansion." Technical report, BRITE/EuRam Project BE-4098, 1994. Report II-34.
- [11] D. Levi-Hevroni, A. Levy, and I. Borde. "Mathematical modeling of drying of liquid/solid slurries in steady state one-dimensional flow." *Drying Technology*, vol. 13, 1995, pp. 1187-1201.
- [12] D.R. Shaver, S.P. Antal, M.Z. Podowski, and D. Kim. "Direct steam condensation modeling for a passive PWR safety system." OECD Nuclear Energy Agency and IAEA Workshop, Washington, D.C., Sept. 2010.
- [13] CD-Adapco. "Star-CD version 4.14 methodology manual." 2010.

- [14] Akio Tomiyama, Hidesada Tamai, Iztok Zun, and Shigeo Hosokawa. "Transverse migration of single bubbles in simple shear flows." *Chemical Engineering Science*, vol. 57, 2002, pp. 1849-1858.
- [15] D.G. Karamanev. "Rise of gas bubbles in quiescent liquids." *AIChE Journal*, vol. 40, issue 8, 1994, pp. 1418-1421.
- [16] D. A. Drew and R. R. Lahey Jr. "The virtual mass and lift force of a sphere in rotating and straining inviscid flow." *International Journal of Multiphase Flow*, vol. 13, issue 1, 1987, pp. 113-121.
- [17] M. Lopez de Bertodano, RT Lahey, and OC Jones. "Phase distribution in bubbly two-phase flow in vertical ducts." *International Journal of Multiphase Flow*, vol. 20, issue 5, 1994, pp. 805-818.
- [18] W. Yao and C. Morel. "Volumetric interfacial area prediction in upward bubbly two-phase flow." *International Journal of Heat and Mass Transfer*, vol. 47, issue 2, 2004, pp. 307-328.
- [19] S. Hosokawa and A. Tomiyama. "Multi-fluid simulation of turbulent bubbly pipe flows." *Chemical Engineering Science*, vol. 64, 2009, pp. 5308-5318.
- [20] SP Antal, RT Lahey Jr, and JE Flaherty. "Analysis of phase distribution in fully developed laminar bubbly two-phase flow." *International Journal of Multiphase Flow*, vol. 17, issue 5, 1991, pp. 635-652.
- [21] BE Launder and BI Sharma. "Application of the energy-dissipation model of turbulence to the calculation of flow near a spinning disc." *Letters Heat Mass Transfer*, vol. 1, 1974, pp. 131-137.
- [22] BE Launder and DB Spalding. "The numerical computation of turbulent flows." *Computer Methods in Applied Mechanics and Engineering*, vol. 3, issue 2, 1974, pp. 269-289.
- [23] B. E. Launder, A. Morse, W. Rodi, and D. B. Spalding. "Prediction of free shear flows: a comparison of the performance of six turbulence models." Technical report, NASA, 1973. Document ID: 19730019433.
- [24] W. Rodi. "The prediction of free turbulent boundary layers by use of a two-equation model of turbulence." PhD thesis, University of London, 1972.
- [25] F. Mayinger and YM Chen. "Heat transfer at the phase interface of condensing bubbles." 8th International Heat Transfer Conference, vol 4, 1986, pp. 1913-1918.
- [26] YM Chen and F. Mayinger. "Measurement of heat transfer at the phase interface of condensing bubbles." *International Journal of Multiphase Flow*, vol. 18, issue 6, 1992, pp. 877-890.
- [27] J. Isenberg and S. Sideman. "Direct contact heat transfer with change of phase: bubble condensation in immiscible liquids." *International Journal of Heat and Mass Transfer*, vol. 13, issue 6, 1970, pp. 997-1011.
- [28] O. Zeitoun, M. Shoukri, and V. Chatoorgoon. "Interfacial heat transfer between steam bubbles and subcooled water in vertical upward flow." *Journal of Heat Transfer*, 1995, pp. 117-402.
- [29] G.R. Warriar, N. Basu, and V.K. Dhir. "Interfacial heat transfer during subcooled flow boiling." *International Journal of Heat and Mass Transfer*, vol. 45 issue 19, 2002, pp. 3947-3959.
- [30] RI Nigmatulin, NS Khabeev, and FB Nagiev. "Dynamics, heat and mass transfer of vapour-gas bubbles in a liquid." *International Journal of Heat and Mass Transfer*, vol. 24 issue 6, 1981, pp. 1033-1044.